Desalination and Water Treatment
www.deswater.com
doi: 10.5004/dwt.2023.30139

315 (2023) 327–341
December

Containment of ciprofloxacin and copper in groundwater using nanocomposite prepared by the use of pomegranate peel extract: characterization, kinetic, and modeling study

Ziad Tark Abd Ali[a,*], Noor Alaa Abdulhusain[b]

[a]*Department of Environmental Engineering, College of Engineering, University of Baghdad/Iraq, email: z.teach2000@yahoo.com*
[b]*Environmental Research and Studies Center, Babylon University, Iraq, email: noor.alkufaishi@gmail.com*

Received 3 September 2023; Accepted 10 November 2023

ABSTRACT

The present investigation involved utilizing a green technique to produce nanoparticles (Fe/Pb) using pomegranate peel extract, which they then immobilized using quartz sand (QS) to create a nanocomposite symbolled (QS-Fe/Pb). The prepared nanocomposite was used in the permeable reactive barrier (PRB) technology as reactive materials for the treatment of groundwater contaminated with ciprofloxacin (CIP) and copper (Cu(II)) in batch mode. This barrier was evaluated theoretically by creating a two-dimensional aquifer model solved via the COMSOL Multiphysics 3.5a program. The nanocomposite was characterized through many tests, which included X-ray diffraction, surface area analysis, Fourier-transform infrared spectroscopy, transmission electron microscopy, scanning electron microscopy, and energy-dispersive X-ray spectroscopy. A number of factors that have an impact on the rate of pollutant removal in the batch mode were also studied to determine the optimal conditions that give the maximum removal rate of about 99%. The study used two isotherm models, Langmuir and Freundlich, three kinetic models, including pseudo-first-order and pseudo-second-order models, and intraparticle diffusion were also used. Results from batch mods showed that Freundlich and pseudo-second-order models were the most consistent, as the adsorption capacities were about 9.8 and 15 mg/g for copper and ciprofloxacin, respectively. Furthermore, the results obtained from the two-dimensional aquifer model demonstrate that the nanocomposite material under investigation exhibits promising potential as a reactive medium in the context of PRB technology. This is attributed to its ability to effectively impede the propagation of ciprofloxacin and copper ions (Cu(II)).

Keywords: Green synthesis of nanocomposite; Copper; Ciprofloxacin; Groundwater remediation

1. Introduction

Antibiotics play a crucial role in contemporary medicine for humans and animals, having been formulated to elicit desirable or advantageous effects on microorganism-related ailments [1]. Antibiotics play a vital role in modern veterinary medicine [2]. Ciprofloxacin, commonly called CIP, is one of the most extensively employed antibiotics [3]. This compound is a member of the third generation of the quinolone pharmacological class [4]. The extensive application of this substance can be attributed to its chemical stability and potent antibacterial properties, which have also been observed in aquatic ecosystems. Many bacterial infections are treated with the fluoroquinolone antibiotic (ciprofloxacin). Its presence was identified in numerous water systems [5,6]. Copper(II) is an essential element in the heavy metal sector, and it is extensively employed in various applications, used in petroleum refining, brass manufacturing, as

* Corresponding author.

well as plating, etc. The presence of copper(II) in the environment is attributed to tailings from mining, smelting, and processing of copper ore. The condition under consideration has been found to result in a range of developmental anomalies and pathological conditions in the human population [7]. The urgent need for a clean environment for humans has led to a focus on developing efficient methods of eliminating the combination of organic chemicals and toxic metals, the most prevalent form of contamination of the environment worldwide [8].

Groundwater is generally considered a more reliable water source for human consumption compared to surface water in most cases. However, it remains susceptible to pollution as chemical compounds possess high solubility and can permeate the soil, ultimately reaching the groundwater and causing pollution [9]. Pumps and treat, permeable reactive barrier (PRB), and *in-situ* flashing, are only a few methods to remediate polluted groundwater [10,11]. The reactive substance discovered deep in the soil and close to the source of pollution is what the PRB technique relies by the study of Al-Hashimi et al. [12] and Abd Ali & Ismail [13]. The potential of employing various reactive materials, including graphene glass/sand hybrid, cement kiln dust, zero-valent iron, and others, in the restoration of polluted groundwater has been investigated by several researchers [14–16]. It remains necessary to develop an absorbent (reactive goods) with a high efficacy rate that is effective, economical, and produced in green ways without any adverse side effects on the environment.

In this study, a reactive substance (nanocomposite) was prepared and utilized in PRB technology to eliminate groundwater pollutants by utilizing a green method that utilizes agricultural waste extract as an anti-oxidant instead of chemicals harmful to the environment. Because of its abundant supply, cheap cost, and high-level content of polyphenol compounds, agricultural waste has lately been investigated to be utilized as a green antioxidant or sorbent for eliminating organic and inorganic debris in either its original form or an enhanced version. Pomegranate peel is a good candidate for reduction-based nanomaterial production since it has anti-oxidant capabilities [17].

Antibiotics and heavy metals are only two toxins that may be removed from the environment using nano zero-valent iron (nZVI)-based treatment methods. Rapid aggregation, low stability, and inadequate separation from the reactants are some drawbacks of the nZVI. The nZVI particles are often enhanced in various ways [18], such as emulsifying the particles, doping them with extra metal, treating the surface with a chemical stabilizer, and introducing support material. Some noble metals, such as "Cu" [19], "Ag" [20], "Pt" [18], "Ni" [21], and "Pd" [22] have been used in trace amounts with nZVI to form bimetallic particles [23], in addition the "Pb" was used for the first time in our previous works [24,25]. These metals act as catalysts, thus enhancing the ability of the zero-valent iron nanoparticles to remove these pollutants [17]. These metals play dual roles as catalysts and inhibitors. Additionally, it promotes the generation of H_2 close to the surface of nano zero-valent iron [26], boosting iron nanoparticles' reactivity, and aids in lowering the activation energy while increasing decreasing energy [27].

The main idea of this study was to combine lead as dopant metal with zero-valent iron to produce bimetallic nanoparticles. In addition, pomegranate peel extract was used as an antioxidant instead of other chemicals, including borohydride, to generate nanoparticles that do not threaten the environment was noteworthy. Directly utilizing Fe/Pb nanoparticles in commercial applications would incur significant costs. Additionally, the use of unmodified nanoparticles for contaminant removal would impede the reactant's ability to regenerate and be reused. To overcome these limitations, it is possible to provide an inert material or support system for the particles. The utilization of sand as an inert and supportive material for immobilizing Fe/Pb nanoparticles is attributed to its inert nature and ability to supply exceptional support. This is because surface particles generate delicate layers on the sand surface, rendering it an ideal substrate [28]. The primary objectives of this study were to develop a new type of nanocomposite synthesized using a green method, to be utilized as a reactive material in PRB technology that can eliminate ciprofloxacin and copper from polluted groundwater, and use a hypothetical case solved by COMSOL Multiphysics 3.5a (2008) software to evaluate the efficiency use of the prepared QS-Fe/Pb nanocomposite as a successful reactive material in remediation of contaminated groundwater.

2. Materials and methods

2.1. Materials

The nanoparticles were immobilized and supported using quartz sand (QS) as the matrix, it was procured from a nearby marketplace, with an initial porosity is recorded as 0.45, particle size range from 0.3 to 0.5 mm, additionally, its specific gravity is measured at 1.363. The absolute chemicals ethanol (99.9%), ($Cu(NO_3)_2{\cdot}3H_2O$) as copper(II) nitrate, lead sulfate ($PbSO_4$), and ferric chloride ($FeCl_3$) were procured from HSC, Germany. The compound ciprofloxacin ($C_{17}H_{18}FN_3O_3$) was obtained from Samarra Pharmaceutical Factory, Iraq. The chemicals and reagents utilized in the experiment were of analytical-grade quality.

2.2. Preparation of reactive material (nanocomposite)

The initial stage of preparing the reactive material involved the synthesis of pomegranate peel extract. Pomegranate fruit was bought from a local vendor, subjected to cleansing with tap water, and manually peeled. The peels were dried in an oven for 40 h at 60°C. Following this, an extraction process was carried out using ethanol (10%) within a shaking incubator for 25 h. The filtrate was obtained and stored at 20°C for potential future use. The nanocomposite was synthesized using the green synthesis method outlined by the study of Ravikumar et al. [28]. By this procedure, a quantity of 100 g of QS was combined with 150 mL of a 0.1 molar solution of $FeCl_3$. The resulting mixture was subsequently agitated on an orbital shaker for half an hour to achieve uniform $FeCl_3$ solution and QS distribution. Later, the sand coated with Fe was desiccated for one night in a vacuum oven maintained at 80°C. A 10% solution

of pomegranate peel extract was cautiously introduced to sand coated with $FeCl_3$ that had been dried. This resulted in a noticeable alteration in the color of the mixture from a golden yellow hue to a black shade. The emergence of a black precipitate signifies the formation of Fe(0) nanoparticles, as cited in previous literature [28,29]. The pomegranate peel extract was added to the mixture and maintained on an orbital shaker for half an hour at room temp to ensure uniform mixing. A 150 mL solution of 0.1 M $PbSO_4$ was added to the mixture, and the shaking time was increased to 1 h. The resulting nanocomposite was filtered, washed thrice with 100% ethanol, and dried in an 80°C vacuum oven. It was stored in a sealed container for utilization in subsequent batches and ongoing experiments. Fig. 1 depicts a visual abstract of the green-synthesis process of producing the (QS-Fe/Pb) nanocomposite [28,29].

2.3. Characterization of nanocomposite

Before its utilization in experimental investigations, the composite material (QS-Fe/Pb) was subjected to multiple analyses to assess its characteristics: such as the X-ray diffraction (XRD) analysis that confirmed the synthesized composite's crystallinity, scanning electron microscopy (SEM) was employed to measure the specific surface area, a crucial parameter in assessing the efficacy of adsorbent materials. Brunauer–Emmett–Teller performance was employed, Fourier-transform infrared spectroscopy (FTIR) test to identifying the functional groups of presents on the surface of the active substance responsible for eliminating the pollutants.

The quartz sand and synthesis nanocomposite morphology was analyzed utilizing a Morgagni-270-D transmission electron microscope. The estimation of the transmission electron microscopy (TEM) involved the application of a specimen's solution onto Formvar-coated C grids through dabbing, SEM test also employed to examine the morphology of both quartzes sand and synthesis composites. Additionally, an energy-dispersive X-ray spectroscopy (EDX) examination was utilized to identify the fundamental composition of the produced composite materials.

2.4. Batch experiments

The identification of optimal batch situations for removing pollutants was achieved through the execution of batch studies on ciprofloxacin and copper sorption equilibrium data. The aforementioned conditions encompass a multitude of factors, including but not limited to the duration of contact, pH level of the initial solution, and quantity of synthesis nanocomposite administered. The experimental methodology employed the subsequent procedure: the experimental procedure involved introducing 50 mL of ciprofloxacin and copper solutions, each with an amount of 50 mg/L, into

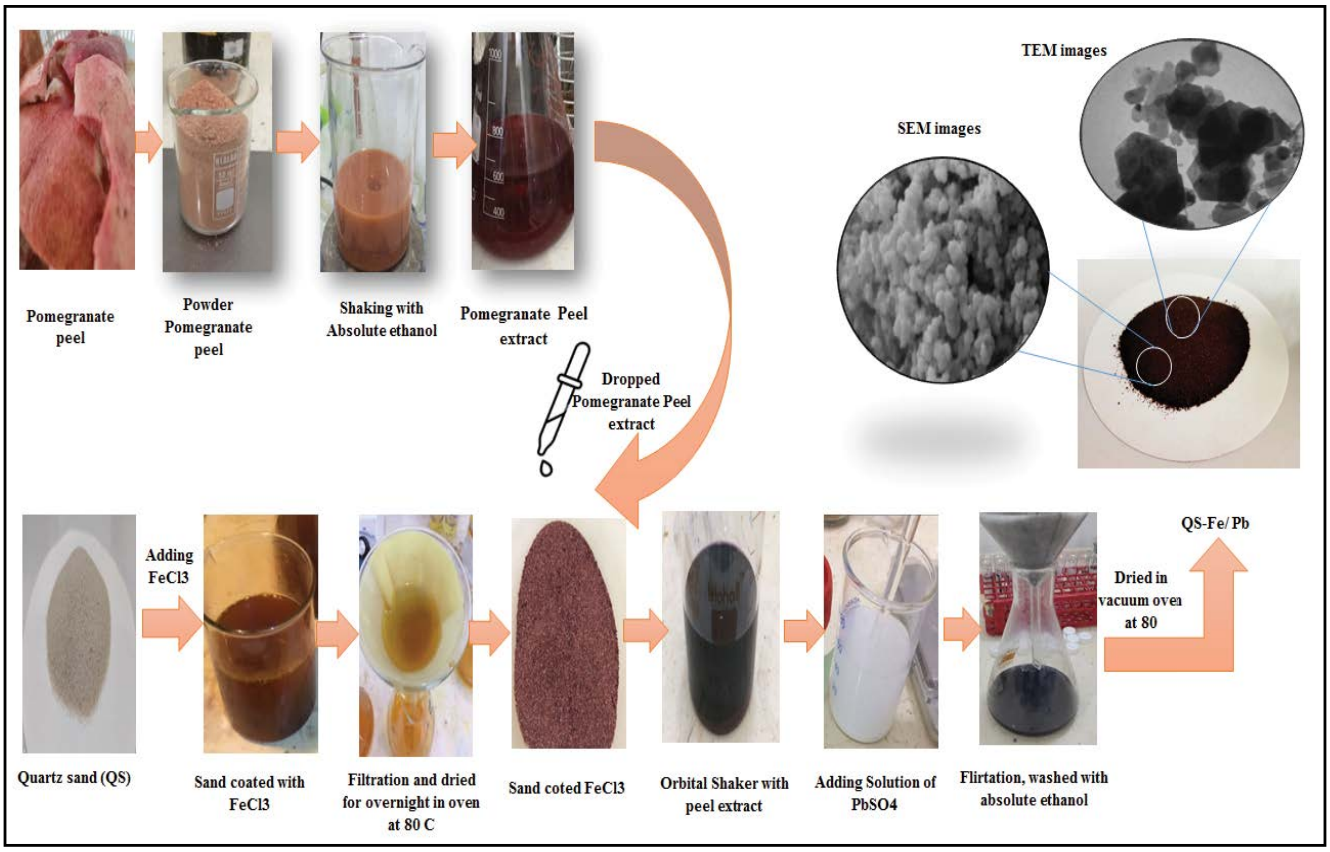

Fig. 1. Graphical abstract of the synthesis of QS-Fe/Pb nanocomposite.

individual 250 mL flasks. Subsequently, 0.2 g of the synthesis composite was added to each flask. Following a 3-h stirring period at 200 rpm, the flasks containing the adsorbent, CIP, and Cu(II) pollutants solutions underwent filtration to isolate the transparent pollutants solution from the remained solid material. 10 mL of each filtered sample for ciprofloxacin and copper were measured. The utilization of atomic absorption spectroscopy was employed to investigate the properties of Cu(II), while the evaluation of the CIP was conducted by applying UV-Visible spectroscopy. To ensure the precision of the results, each specimen underwent three rounds of re-examination. The pH ranges varied from 2–12 for ciprofloxacin and from 2–7 for copper. The absorption process was evaluated using different doses of the nanocomposite, ranging from 0.05 to 1 g/50 mL, with time intervals between 0 and 180 min. To achieve optimal experimental outcomes, the utilization of Eqs. (1) and (2) was implemented to compute the percentage of removal (R%) and the amount of pollutants that were retained in the solid phase (q_e) [15,30].

$$R\% = \frac{C_o - C_t}{C_o} \times 100 \tag{1}$$

$$q_e = \frac{C_o - C_e}{m} V \tag{2}$$

where C_o initial contaminants amounts (mg/L), C_e equilibrium contaminants amounts (mg/L) in the flask, m is the QS-Fe/Pb mass composite in the flask (g), and V is the solution volume in the flask (L).

2.5. Distilled water leaching test

The utilization of prepared nanocomposite as a reactive substance in permeable reactive barrier technology necessitates verifying its capacity to retain the selected pollutants for an extended duration and prevent their transition into a liquid phase. The two pollutants-bearing QS-Fe/Pb nanocomposite samples underwent a distilled water leaching process by the "German Standard Methods" [31]. The analysis of leachates was conducted to determine the presence of ciprofloxacin and copper.

2.6. Isotherm models

The isotherm models used in this section [32,33]:

- ***Freundlich model***: The model's general formula can be expressed as explained by the study of Sulaymon and Abd Ali [34] however, the utilization of this approach is suitable for surfaces that exhibit heterogeneity and for sorption processes that involve multiple layers [35].

$$q_e = K_f \left(C_e\right)^{1/n} \tag{3}$$

The variable K_f represents the maximum quantity of sorbed solute onto reactive material, while the value 1/n (where n is less than 1) denotes the sorption intensity.

- ***Langmuir model***: The current model applies to the sorption of single-layer and homogeneous surfaces [36]. Eq. (4) can be utilized for expressing it [37]:

$$q_e = \frac{q_{\max} b C_e}{1 + b C_e} \tag{4}$$

The variable $q_{\max}$ represents the maximum adsorption capacity (mg/g), while the variable b denotes the intensity of the pollutant with respect to the solid phase.

2.7. Kinetic models

One can estimate this rate by utilizing the kinetic variables listed [38]:

- ***Pseudo-first-order***: The current framework is based on a robust capacity, commonly referred to as demonstrated in Eq. (5) [39]:

$$\frac{dq}{dt} = k_1 \left(q_e - q_t\right) \tag{5}$$

Eq. (5) is subjected to integration, resulting in the derivation of Eq. (6).

$$q_t = q_e \left(1 - e^{-k_1 t}\right) \tag{6}$$

The present study considers the parameters q_e and q_t, denoting the amount of solute (mg/g) adsorbed at equilibrium and at a specific duration t. The pseudo-first-order kinetic model at equilibrium is characterized by a constant rate K_1 (1/min).

- ***Pseudo-second-order***: This model can be mathematically represented in Eq. (7) [40,41]:

$$\frac{dq}{dt} = k_2 \left(q_e - q_t\right)^2 \tag{7}$$

The rate constant of the second model is denoted as K_2 (g/mg·min) in the context. To obtain the second equation in nonlinear forms, it is necessary to integrate Eq. (8):

$$q_t = \frac{t}{\left(\frac{1}{k_2 q_e^2} + \frac{t}{q_t}\right)} \tag{8}$$

The utilization of the aforementioned two kinetic models is inadequate in providing a comprehensive understanding of the prevailing mechanisms. Consequently, another model was employed:

- ***Intraparticle diffusion***: This model is represented by Eq. (9):

$$q_t = k_{\text{int}} t^{0.5} + C \tag{9}$$

The variable "k_{int}" in the diffusion model represents the sorption rate constant, expressed in units of mg/g·min$^{0.5}$.

Meanwhile, the intercept "*C*" provides information about the thickness of the boundary layer.

2.8. Two-dimensional aquifer model

In order to ascertain the viability of utilizing the prepared nanocomposite, which was synthesized in the present investigation, as an efficacious reactive substance in the context of PRB method for remediation groundwater that has been polluted with ciprofloxacin and copper, the synthesis nanocomposite was employed as a reactive barrier in a hypothetical scenario involving a two-dimensional aquifer model. The present study employs a numerical approach to investigate the migration behavior of ciprofloxacin and copper in a flow two-dimensional field. The finite element technique is utilized for solving the simulation, and the COMSOL Multiphysics 3.5a software is employed. The current research outlines a theoretical simulation for treating groundwater polluted with (CIP and Cu(II)) utilizing PRB technology. The simulation employs a two-dimensional aquifer model, wherein COMSOL 3.5a facilitates the simulation. Specifically, the simulation incorporates one-dimensional flow (advection) in the *X*-direction and two-dimensional solute transport (dispersion) in the *X* and *Y*-directions across an unconfined aquifer. The current simulation employed a unidirectional fluid flow solely in the *X*-direction, despite a transverse component in the flow velocity in the *Y*-direction. This approach is deemed appropriate for the scenario stated by the study of Khebchareon [42]. This study formulates a model for estimating the spatial and temporal extent of the sub surface's CIP and Cu(II) plume. The aquifer model is confined within a square shape measuring 50 m × 50 m, as depicted in Fig. 2. The aquifer model suggested in the QS-Fe/Pb-PRB study comprised three distinct components. The initial segment of the aquifer model was composed of a 30-m stretch of sandy soil on the left-hand side. Between sections 1 and 3 of the aquifer models, the subsequent section was a 3-m thick PRB. The final segment of the aquifer model was composed of 17 m of sandy soil on the right-hand side. The experiment involved introducing CIP and Cu(II) solutions, with an initial amount of 0.05 kg/m^3 and a velocity of 0.48 cm/min, into a model aquifer through a line source on the left side of the aquifer, spanning a length of 10 m. The aforementioned line source emulated an uninterrupted discharge of pollutants. The concentrations of CIP and Cu(II) at interest points were monitored in front of (inflow), within (different thickness), and behind (outflow) the PRB. The boundaries and initial conditions of the two-dimensional solute transport modeling are explained in Table 1. It is clear that the initial condition corresponds to the situation where the contaminants are initially absent from the two-dimensional porous formation, except in the line source described.

2.9. Transport of Cu(II) and CIP through the aquifer model

The one-dimensional advection-dispersion formula can describe contaminants' transport in porous media, as shown in Eq. (10). As per the given equation, the governing factors responsible for transporting dissolved contaminants have been sorption, advection, and dispersion. Dispersion refers to the movement of contaminants resulting from the amount of gradients and diverse pathways, whereas advection pertains to the contaminant migration alongside flowing water [43].

$$D_x \frac{\partial^2 C}{\partial x^2} - V_x \frac{\partial C}{\partial x} = \frac{\partial C}{\partial t} + \frac{\rho_b}{n} \frac{\partial (q)}{\partial t} \tag{10}$$

The variables in the equation above are defined: *n* represents the porosity of the porous medium, *V* denotes the velocity of pore water measured in meters per minute, *q* signifies the sorbed amount of pollutants onto the sorbent substance measured in mg/g, *D* represents the hydrodynamic

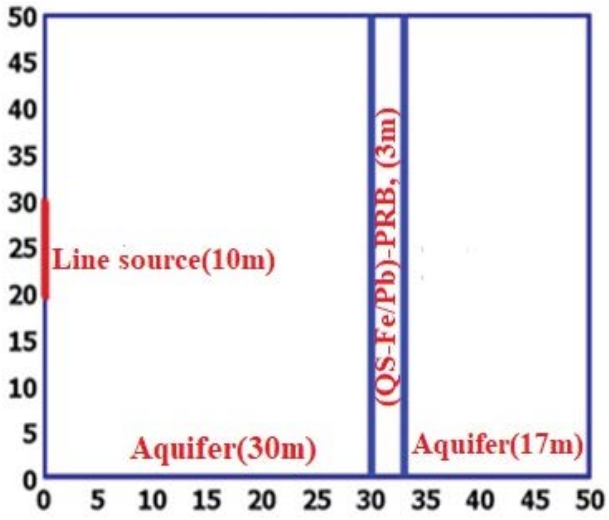

Fig. 2. Two-dimensional aquifer model used for simulation of CIP and Cu(II) transport.

Table 1
Boundaries and initial conditions used in the two-dimensional model set-up

Item	Location	Type/Value	
Boundary settings	Upper boundary	No flux/symmetry	
	Lower boundary	No flux/symmetry	
	Left side boundary	Line source	C_o = 0.05 kg/m^3
		Except for the line source	No flux/symmetry
	Right side boundary	Advective flux = 0	
Initial condition	(*X*, *Y*)	Initial concentration = 0	

dispersion coefficient, and ρ_b represents the bulk density measured in kg/m^3. The expression $\frac{\rho b}{n}\frac{\partial(q)}{\partial t}$ denotes the alteration rate in the amount of the pollutants solution caused by sorption mechanisms. Here, q represents the amount of the pollutants (Cu(II), CIP) that have been sorbed on the reactive media (QS-Fe/Pb nanocomposite). Therefore, the expression, as mentioned earlier, can be formulated subsequently.

$$\frac{\rho b}{n}\frac{\partial(q)}{\partial t} = \frac{\rho b}{n}\left(\frac{dq}{dc}\frac{\partial C}{\partial t}\right) \tag{11}$$

Incorporating the description of variable q into Eq. (10) provides by Eq. (12):

$$D_x\frac{\partial^2 C}{\partial x^2} - V_x\frac{\partial C}{\partial x} = R\frac{\partial C}{\partial t} \tag{12}$$

The variable R denotes the impact of the sorption process on the deceleration of pollutants transport. The parameter in question is commonly referred to as the factor of retardation and its estimation can be derived using Eq. (13):

$$R = 1 + \frac{\rho b}{n}\frac{\partial q}{\partial C} \tag{13}$$

Eq. (12) is employed to represent the transport of contaminants in porous media in a one-dimensional context. However, it can be modified to depict the transport of contaminants in a two-dimensional context, as demonstrated in Eq. (14):

$$D_x\frac{\partial^2 C}{\partial x^2} + D_y\frac{\partial^2 C}{\partial y^2} - V_x\frac{\partial C}{\partial x} = R\frac{\partial C}{\partial t} \tag{14}$$

The present investigation has assigned an R-magnitude of 1 for the percolation of groundwater polluted with (Cu(II)/CIP) thru sandy soil (aquifer). This value is deemed appropriate for such soil types, typically regarded as non-reactive or inert media. The sorption process of Cu(II)/CIP using synthesis nanocomposite (QS-Fe/Pb) was depicted in the aquifer model *via* the isotherm model that corresponds with the batch experimental data, as evidenced by a more significant determination coefficient (R^2). The numerical solution of two-dimensional aquifer model, as described by Eq. (14) and subject to the initial and boundary conditions outlined in Table 1, was obtained using COMSOL Multiphysics 3.5 software. This software is founded upon the technique of finite elements.

3. Results and discussion

3.1. Characterization of the prepared composite

Fig. 3 depicts the XRD spectral data of the prepared nanocomposite material both before and after its reaction with Cu(II) and CIP. The data presented in this figure demonstrates the presence of notable diffraction peaks occurring at 2θ values of 68.475°, 60.325°, 50.475°, and 42.775°. These peaks indicate the generation of Fe/Pb nanoparticles on the surface of the sand, as previously reported in the literature [44]. The intensity at the peak value of 60.325 exhibited a notable reduction after interacting with CIP, which can be attributed to the redox process between ciprofloxacin and synthesis composite. The reflections denote the novel locations on the surface of the sand that transformed the inactive sand into a responsive substance [38]. Subsequently, a reduction was observed following the reaction of synthesis composite with copper at the peak (75.975). The variances in the crystallinity and phase of nanocomposite during Cu chemisorption could account for the observed XRD patterns of the material pre- and post-adsorption [45].

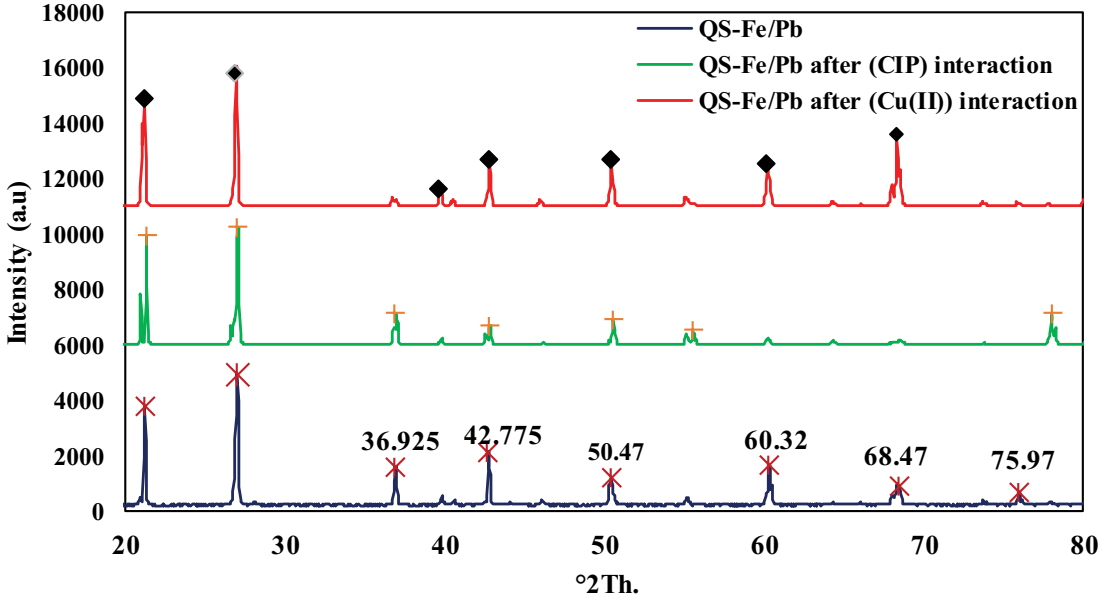

Fig. 3. X-ray diffraction test for QS-Fe/Pb nanocomposite before and after interaction with CIP and Cu(II).

The surface area of synthesis composite was observed to be substantially greater than that of QS, with values of 6.0488 and 0.56233 m^2/g, respectively. The pore volume of sand was found to be 0.003829 cm^3/g, and subsequent coating with nanoparticles increased to 0.008355 cm^3/g. The observed augmentation in surface area and pore volume of synthesis composite (QS-Fe/Pb) could be attributed to nanoparticle deposition onto the sand's surface. The results of this examination are consistent with the discoveries made by other scholars, as cited by Ravikumar et al. [28].

Fig. 4 presents the FTIR spectral assessment of QS-Fe/Pb within the 400–4,000 cm^{-1} range. The polyphenol amount in the pomegranate peel extract is directly associated with the vibratory stretching of the O–C–O and C=C functional sets that manifest as multiple peaks at 2,351; 2,150 and 1,632 cm^{-1}. This finding has been reported in previous research [46]. The results indicate that the bio-organic compounds in the fruit peel extract were responsible for the accumulation of Fe/Pb on the sand. This finding is consistent with previous studies that have demonstrated the production of Fe–Ni particles through pomegranate peel extract [26]. The findings indicate that the adsorption of ciprofloxacin and copper by synthesis composite is supported by the FTIR spectrum measurements, as depicted in Fig. 4. The presence of adsorbed selected pollutant on the surface of QS-Fe/Pb is supported by the observed peaks at 3,416; 1,874 and 1,156 cm^{-1} for ciprofloxacin and 3,416 and 1,095 cm^{-1} for Cu, as reported by the study of Ravikumar et al. [26].

Fig. 5 illustrates the TEM images of the QS and QS-Fe/Pb composite. The evidence presented in Fig. 5A indicates that the sand is comprised of individual particles without any discernible substructures, thereby demonstrating the absence of any coating on the surface of the sand. The presence of these fragments provides evidence that the Fe/Pb nanoparticles had been effectively applied onto the sand substrate. However, it should be noted that Fig. 5B depicts the formation of discrete particles, which differ significantly from those observed in Fig. 5A.

Fig. 6 displays the SEM images and analysis results (EDX) of quartz sand and synthesis composite (QS-Fe/Pb). The study found that the average diameter of Fe/Pb nanoparticles on the sand surface was 56.97 nm, with a predominant spherical shape. Additionally, the presence of both Pb and Fe on the surface of the sand was confirmed through QS-Fe/Pb EDX analysis.

3.2. Operating conditions in batch mode

The calculation of equilibrium time holds significant importance in batch tests. In this experiment, the interaction time ranged from 5 to 180 min under specified experimental conditions, as depicted in Fig. 7A. The findings indicate that the maximum percentage of removal (70% and 60%) was predominantly attained after 120 and 70 min for Cu(II) and CIP, respectively. The observed rise in the two contaminants removal percentage over time can be attributed to the presence of composite sites that were specifically designated for the sorption of ciprofloxacin and copper. However, as the availability of these sites diminished, the rate of sorption reduced, particularly after 120 and 70 min for Cu(II) and CIP, respectively. This finding has been documented in previous research. The elimination percentage remained relatively

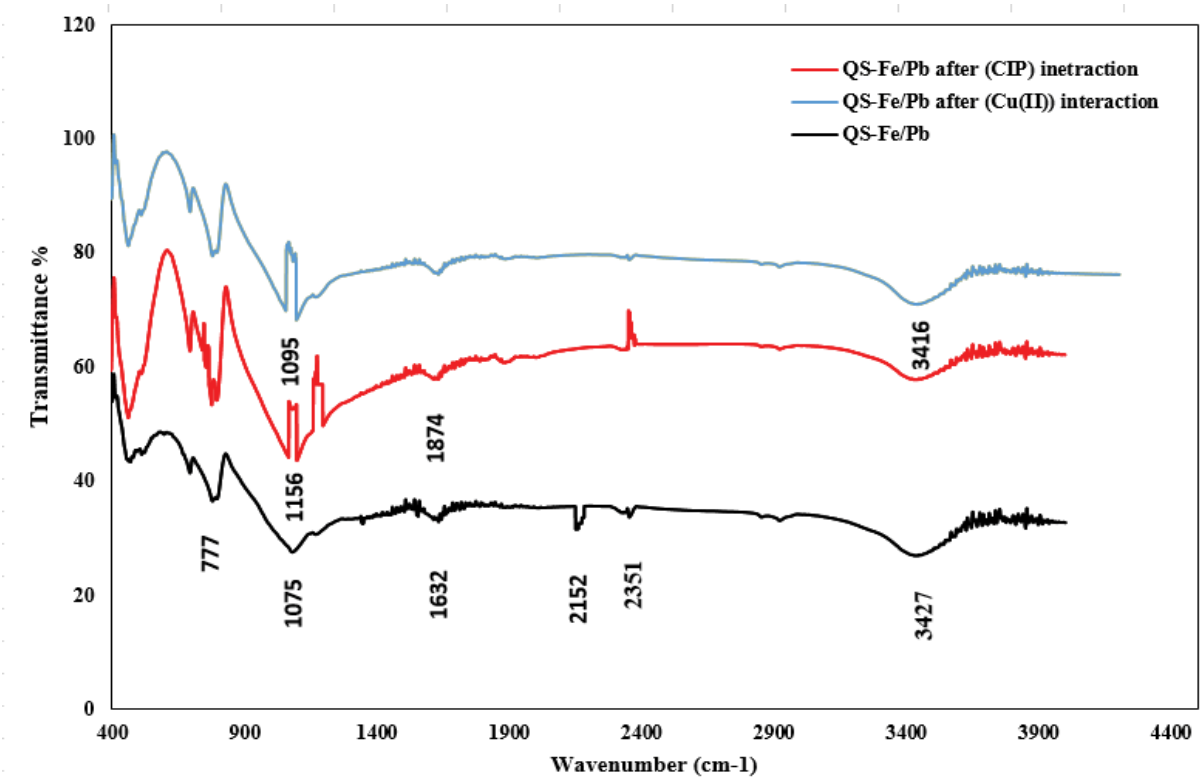

Fig. 4. Fourier-transform infrared spectroscopy analysis for QS-Fe/Pb nanocomposite before and after interaction with CIP and Cu(II).

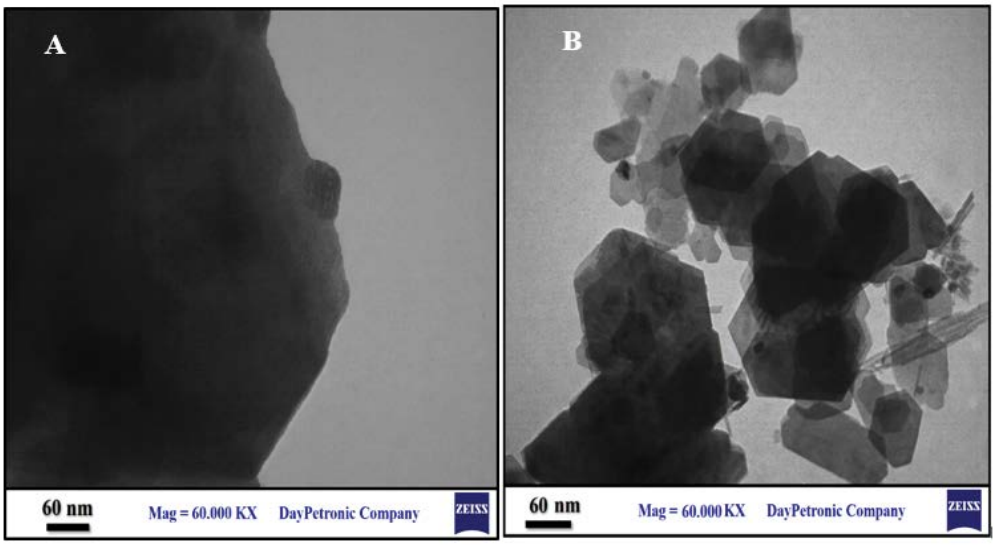

Fig. 5. Transmission electron microscopy images for (A) quartz sand and (B) QS-Fe/Pb nanocomposite.

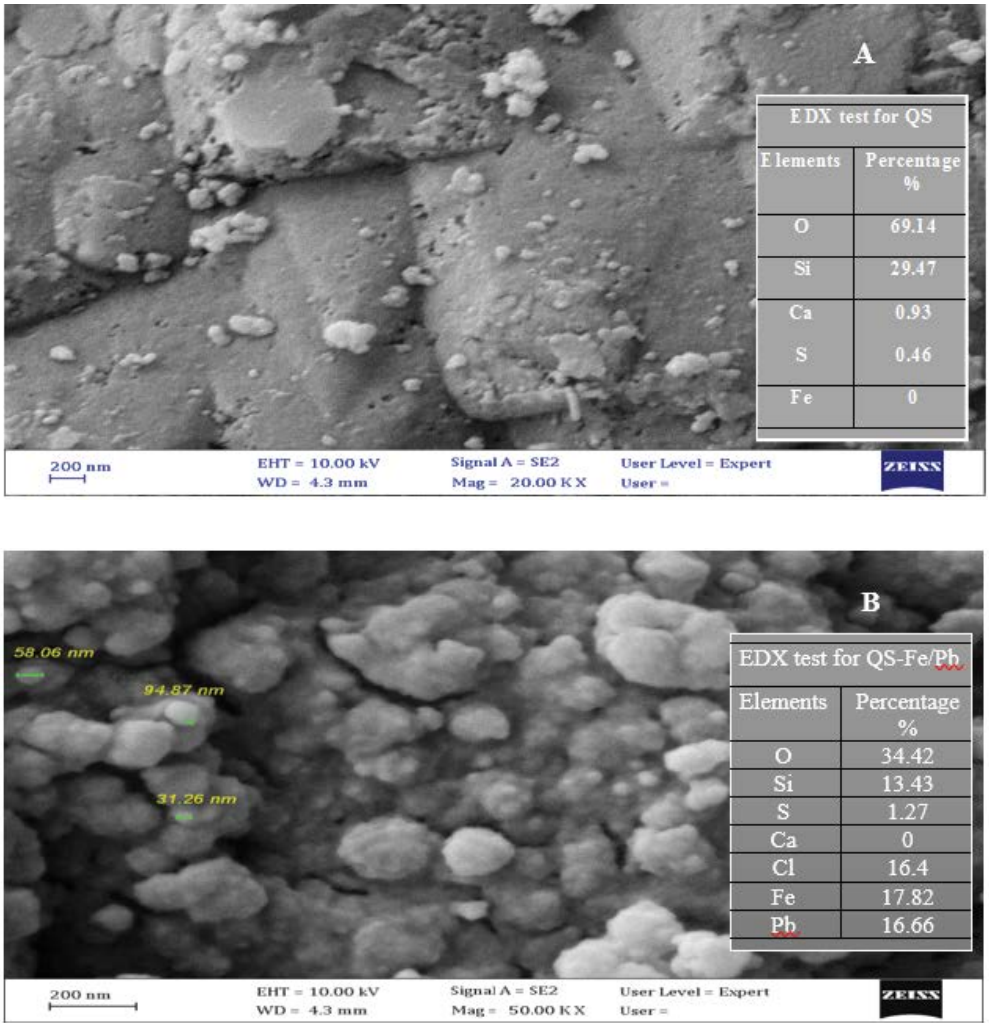

Fig. 6. Scanning electron microscopy images and energy-dispersive X-ray spectroscopy test for (A) quartz sand and (B) QS-Fe/Pb nanocomposite.

stable up to 180 min before attaining equilibrium, indicating that the optimum times for achieving equilibrium state for CIP and Cu(II) are 70 and 120 min, respectively [47].

The inclusion of pH measurements is a crucial aspect to be considered in this investigation, as it significantly impacts the efficacy of CIP and Cu(II) elimination within the aqueous domain. To achieve this objective, it is imperative to conduct tests employing predetermined initial pH intervals ranging from 3 to 7 for Cu(II) and 3 to 12 for CIP while utilizing operational parameter values as illustrated in Fig. 7B. The results indicate that an increase in the initial pH magnitude from 3 to 6 and 7 for Cu(II) and CIP resulted in a corresponding increase in the percentage of pollutants removed. The optimal pH values for achieving the highest removal percentages were found to be 6 and 7 for Cu(II) and CIP, respectively, with removal percentages of 74% and 60%.

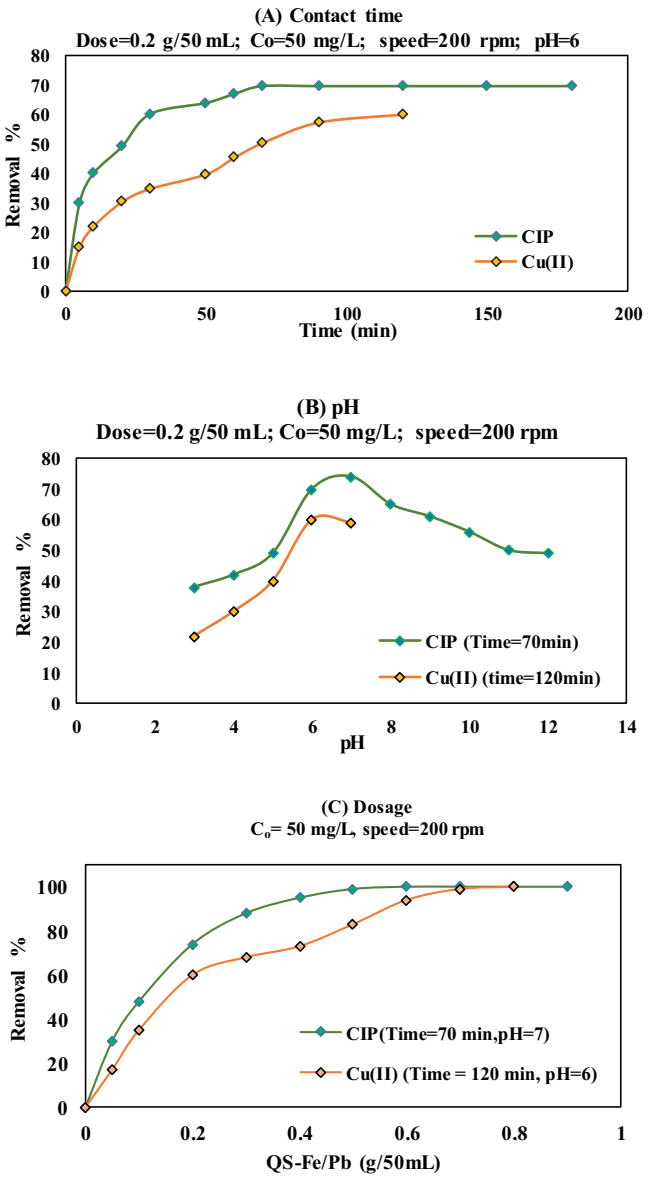

Fig. 7. Removal percentage of CIP and Cu(II) at different condition: (A) contact time, (B) pH, and (C) dosage of QS-Fe/Pb.

However, beyond these optimal pH values, the percentage of pollutants removed percentages reduced as the initial pH value increased. This finding is consistent with previous studies, such as the one conducted by the study of Liu et al. [48]. The observed phenomenon can be characterized: as the pH ranges of 2–6 and 2–7 for Cu(II) and CIP, respectively, increase, the percentage of removal also increases. This can be attributed to a reduction in the hindrances to adsorption between the pollutants and the active sites of (QS-Fe/Pb nanocomposite) due to repulsion, which is regulated by the protonation of the nanocomposite [17]. Subsequent to this, the elimination pattern exhibited dissimilarity. An increase in pH levels to 7 and 12 for Cu(II) and CIP resulted in a decrease attributable to the ionization of hydroxyl sets [49].

The study investigated the correlation between the elimination of ciprofloxacin and copper and the synthesis composite (QS-Fe/Pb) dosage quantity. For the experiment, a composite was prepared and utilized in the range of 0.05 to 1 g/50 mL. Each dose was introduced and consistently blended with 50 mL of aqueous pollutants solution under the operational conditions elucidated in Fig. 7C. The findings indicate that the employment of 0.2 g/50 mL of QS-Fe/Pb composite removed just 74% of ciprofloxacin and 60% of copper. An augmentation in the composite dosage up to 0.5 and 0.7 g/50 mL for ciprofloxacin and copper could result in a significant amplification in the elimination rate up to 99%. This is attributed to the escalated quantities of the sorbent material, which offer a more significant number of active sites [2,50]. The removal percentage is not significantly affected by an elevated amount beyond 0.5 and 0.7 g/100 mL of CIP and Cu(II) due to the stabilization of the amount of contaminants that persisted in the aqueous phase. This discovery is in concurrence with the conclusions of numerous scholars [28,46,51].

3.3. Leaching test

The outcomes of the leaching test revealed that the dissolution of Cu(II) and CIP-bearing synthesis nanocomposite material tends to be minimal, with values falling below the limits of identification. The nanocomposite exhibits a robust affinity towards both pollutants, namely CIP and Cu(II), thereby impeding their reversion to a liquid phase during the current experimental situations. In addition, the Fe and Pb concentration was also tested for the same samples to ensure that the Fe and Pb nanoparticles were strongly bonded with other QS-Fe/Pb nanocomposite constituents and did not leach to the bulk solution. The obtained result confirmed that the Fe and Pb concentration is generally below the limits of detection. This test confirmed the efficacy of the produced synthesis nanocomposite (QS-Fe/Pb) material in retaining pollutants, and the constituents of the prepared nanocomposite (QS-Fe/Pb) were strongly bonded with each other making the possibility of becoming the manufactured material a source of contamination with Fe or Pb(II) is weak, thereby establishing its potential for effective utilization in the context of PRB technology as a successful reactive material.

3.4. Real groundwater test

To enhance the reliability and applicability of the study, authentic groundwater was employed to synthesize the

simulated Cu(II) and CIP-contaminated groundwater. The objective was to evaluate the efficacy of nanocomposite in eliminating selected pollutants utilizing two various kinds of water (distilled water and authentic groundwater) in a batch experiment. The experimental situations were optimized based on previous studies, where the greatest elimination percentage was obtained (initial content = 50 mg/L, t = 70 min for CIP and 120 min for Cu(II), pH = 7 for CIP and 6 for Cu(II), agitation speeding = 200 rpm, QS-Fe/Pb amount = 0.5 g/100 mL for CIP and 0.7 g/100 mL for the Cu(II)). The authentic groundwater was extracted from a precise site in the Babil Governorate of Iraq. The elements of this water were investigated at the Environmental and Water Research, Ministry of Science and Technology, to determine its properties before its use in experimentation. The results of this analysis are presented in Table 2. The experiment's findings indicate that the QS-Fe/Pb can eliminate CIP and Cu(II) from authentic groundwater, albeit with reduced efficacy compared to its performance with distilled water. The elimination percentage of CIP and Cu(II) declined to 77% and 72%, respectively, when natural groundwater was employed, as opposed to 99% when distilled water was utilized. The observed outcome can be attributed to the competitive interaction between the CIP and Cu(II) pollutants and the components that initially existed in the groundwater (as listed in Table 2). This competition occurs at the effective sites situated on the surface of QS-Fe/Pb, ultimately reducing the removal percentage. The study found that the efficacy of QS-Fe/Pb in removing contaminants was superior in distilled water compared to natural groundwater. This can be attributed to the absence of additional compounds that could compete with CIP and Cu(II) on the active sites of QS-Fe/Pb in distilled water, unlike in the case of natural groundwater. Consequently, the experimental protocol utilized distilled water to pollute the synthetic groundwater for all subsequent trials.

3.5. Sorption isotherms

The equilibrium outcomes of the sorption test involving the interactions of synthesis nanocomposite (QS-Fe/Pb) with two pollutants have been explicated concerning the models of the previously delineated adsorption isotherms. Table 3 presents a comprehensive list of variables for the aforementioned models. The results of the experiments were utilized to test the models, as depicted in Fig. 8. The Freundlich model exhibits a superior determination coefficient (R^2) compared to the Langmuir model. This indicates that the Freundlich model better fits the data and more precisely characterizes the sorption process. Consequently, it can be inferred that the binding of ciprofloxacin and copper to the surface of synthesis nanocomposite (QS-Fe/Pb) occurs through multi-molecular layers. It can be noted that the maximum adsorption capacity of the prepared nanocomposite (QS-Fe/Pb) was 14.740 and 8.7 mg/g for CIP and Cu(II), respectively, as presented in Table 3. These findings support the applicability of using QS-Fe/Pb as a useful reactive material for the removal of CIP and Pb(II), in comparison with other materials that were used in previous works, as illustrated in Table 4.

3.6. Sorption kinetic

First-pseudo and second-order kinetic models were utilized to create the kinetic models, as depicted in Fig. 9. The application of non-linear regression was employed to analyze kinetic models based on experimental data, utilizing Microsoft Excel 2016. Table 5 presents a comprehensive list of the kinetic model variables, coefficients of determination (R^2), and sum of squares error (SSE) magnitudes. Table 5 presented indicates that the pseudo-second-order model is well-suited to the kinetic sorption data of two pollutants, as evidenced by its superior R^2 and lower SSE magnitudes. Hence, the sorption kinetics of selected pollutants onto the synthesized composite material was of the chemisorption

Table 3
Sorption isotherm models parameters

Model	Parameter	CIP	Cu(II)
Freundlich	K_f (mg/g)(L/mg)$^{1/n}$	4.508	2.27
	n	3.175	2.85
	R^2	0.984	0.967
	SSE	4.606	3.874
Langmuir	q_m (mg/g)	14.740	8.700
	b (L/mg)	0.290	0.120
	R^2	0.932	0.960
	SSE	22.986	7.482

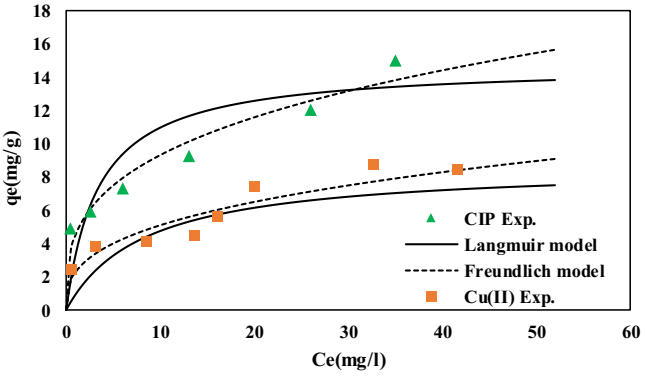

Fig. 8. Isotherm models and experimental data for sorption of CIP and Cu(II).

Table 2
Analysis result of real groundwater

Taste	pH	TDS, ppm	TSS, ppm	SO_4, ppm	Cl, ppm	PO_4, ppm	NO_3, ppm	NO_2, ppm	Ca, ppm	Mg, ppm	K, ppm	Na, ppm	Pb, ppm	Cd, ppm	Cu, ppm	Ni, ppm
Value	7.1	1,236	2.4	491.59	219.52	0.149	1.159	0.069	120	149.32	5.8	190.79	0.0	0.0	0.0759	0.0

Table 4
Comparison of QS-Fe/Pb nanocomposite adsorption capacity with other materials that were used in previous works

Material	Adsorption capacity		References
	CIP	Cu(II)	
Bimetallic iron/nickel nanoparticles		0.2 mg/g	[52]
Polyvinylpyrrolidone stabilized nZVI/Cu	1.16 mg/g		[53]
Zerovalent iron (nZVI) with copper (Cu) bimetallic	0.5 mg/g		[54]
Clay supported Fe/Ni		5 mg/g	[55]
Zerovalent iron (nZVI) with magnesium hydroxide	1.6 mg/g		[56]
Green synthesis of sand-bimetallic Fe/Pb nanoparticles	14.74 mg/g	8.7 mg/g	(Current study)

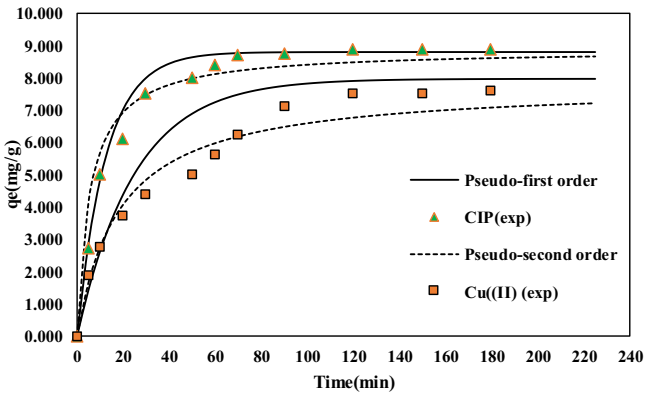

Fig. 9. Kinetic models and experimental measurements for sorption of CIP and Cu(II).

type. The utilization of the intraparticle diffusion model in the evaluation of sorption kinetics measurements demonstrated that $t^{0.5}$ may be associated with q_t in a linear correlation that exhibit an acceptable R^2, as depicted in Fig. 10.

The y-intercepts of the lines in the intraparticle diffusion model indicate the occurrence of intraparticle diffusion in both pollutants ciprofloxacin and copper sorbents, despite not being the rate-controlling step. The three sections about linearity are depicted by the plotted lines, while the sorption process typically entails two or more steps. The magnitude of the rate constant (k) exhibit a higher magnitude for "part 1" in comparison to "portions 2 and 3", as evidenced by the data presented in Table 5. Therefore, controlling the initial segment thru prompt or external surface adsorption is feasible. Table 5 indicates that the rate constant (k), which corresponds to the slopes of the drawn lines, exhibits greater magnitudes for "portion 1" in comparison to "portions 2 and 3". Consequently, the initial segment may be regulated by instantaneous or externally absorbed sorption [35]. Based on the acquired data, it can be inferred that the sorption mechanisms of CIP and Cu(II) on the synthesis composite involve three primary stages, suggesting that intraparticle diffusion does not serve as the rate-limiting step for the overall reaction. The initial stage (portion 1) involves bulk diffusion, followed by the linear phase (portion 2), which is characterized by intraparticle diffusion and culminates in the attainment of equilibrium (portion 3). The magnitudes of K_1, K_2, and K_3 are determined by utilizing the gradients of the straight lines, as presented in Table 5.

Table 5
Resulted parameters of fitting kinetic measurements for sorption of CIP and Cu(II) onto QS-Fe/Pb nanocomposite

Kinetic	Parameter	CIP	Cu(II)
Pseudo-first-order	q_e (mg/g)	8.800	7.970
	q_e Exp. (mg/g)	8.875	7.625
	K_1 (1/min)	0.080	0.040
	R^2	0.97	0.96
	SSE	2.361	10.644
Pseudo-second-order	q_e Exp. (mg/g)	8.875	7.625
	q_e (mg/g)	8.880	7.800
	K_2 (g/mg·min)	0.020	0.007
	R^2	0.987	0.973
	SSE	2.058	2.544
Intraparticle diffusion	Portion 1		
	k_{int} (mg/g·min$^{0.5}$)	1.3983	0.8449
	R^2	0.9788	0.9991
	Portion 2		
	k_{int} (mg/g·min$^{0.5}$)	0.4909	0.6577
	R^2	0.8948	0.9735
	Portion 3		
	k_{int} (mg/g·min$^{0.5}$)	0.0297	0.1167
	R^2	0.6464	0.8307

The hypothesis was made that the sorbent was significantly influenced by the diffusion of the pores and film due to the greater macro pore diffusion compared to micropore diffusion [57]. Linear regression was employed to compute the variables of the models utilizing Microsoft Excel [58]. The rate of the pollutants' sorption process was governed by external mass transfer, whilst diffusion controlled the movement of the lines away from the origin point [16,59].

3.7. Simulation of contaminants (Cu(II) and CIP) transport

The two-dimensional advection–dispersion equation is a proficient and effective method for assessing pollutants' dispersion and advection within the aquifer and PRB system. The current research has utilized the COMSOL Multiphysics 3.5a software to solve the formula, which is deemed precise for the model under consideration. Figs. 11 and 12 present the anticipated contour plot of the modeling outcomes

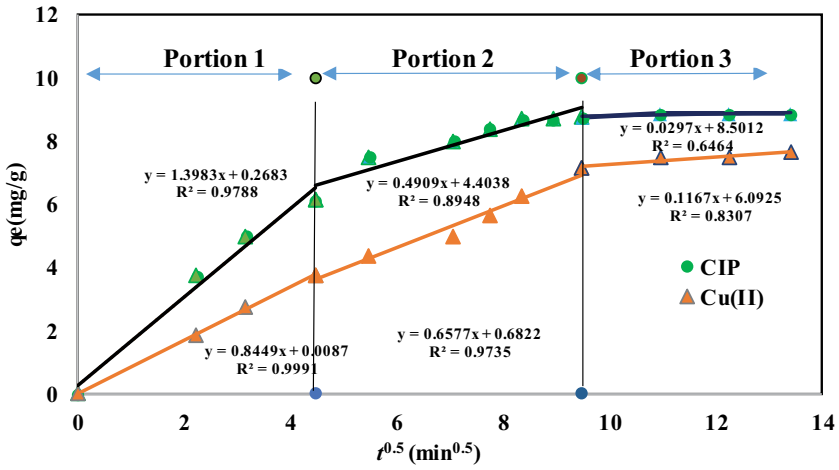

Fig. 10. Intraparticle diffusion model and sorption of CIP and Cu(II) from experimental measurements.

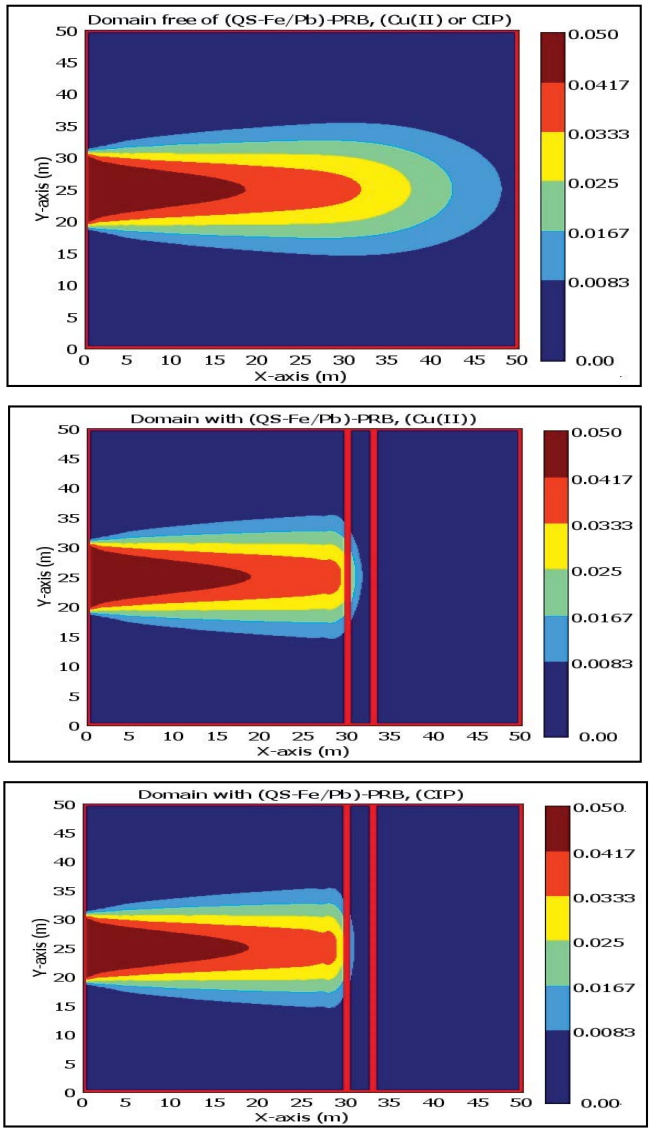

Fig. 11. Contour plot of CIP and Cu(II) concentrations (kg/m³) across the aquifer model after 5 d.

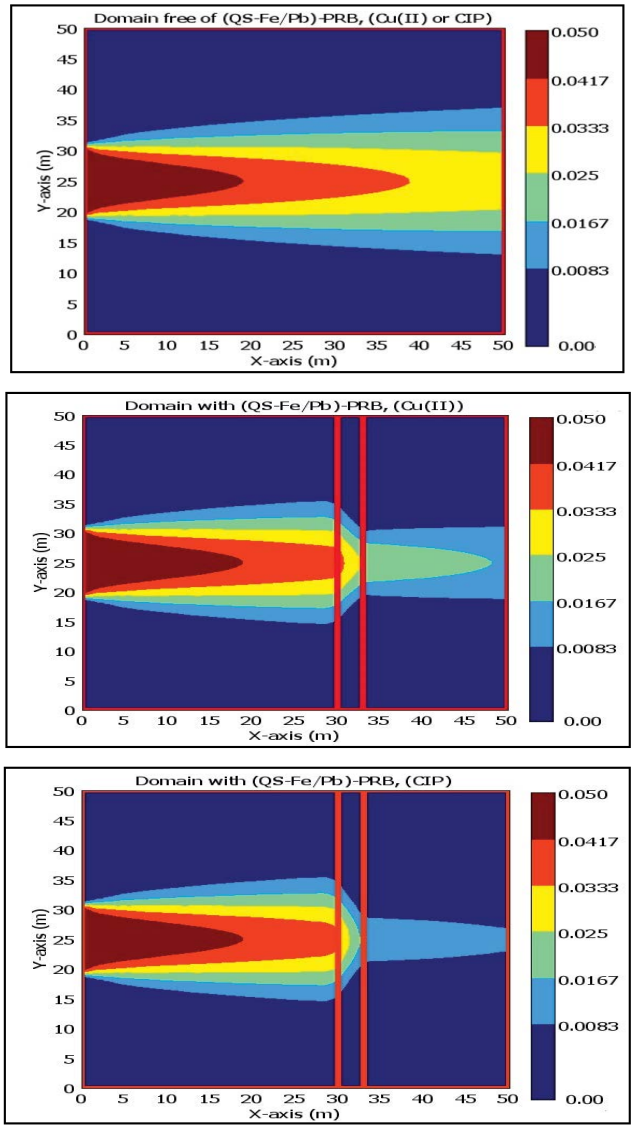

Fig. 12. Contour plot of CIP and Cu(II) concentrations (kg/m³) across the aquifer model after 100 d.

for the transport of contaminants in ciprofloxacin and copper-polluted groundwater, with a Co value of 0.05 kg/m^3 and a velocity of 0.48 cm/min, across the aquifer model in two scenarios: one with a domain that is free of QS-Fe/Pb-PRB and the other with an environment that includes QS-Fe/Pb-PRB. The results are shown after 5 and 100 d, respectively. The transport process of two pollutants (CIP and Cu(II)) is influenced by advection and dispersion, resulting in a directional flow from a high amount gradient on the left-hand side to a lower amount gradient on the right-hand side. The presence of QS-Fe/Pb-PRB impedes the pollution plume, leading to a lower concentration of contaminants reaching the aquifer outlet in the domain with QS-Fe/Pb-PRB compared to the environment without it. The QS-Fe/Pb-PRB significantly hinders the advancement of the CIP relative to Cu(II) in the barrier zone, given equivalent velocity and travel duration. The observed phenomenon can be explained by the varying affinities of CIP and Cu(II) towards the binding sites of QS-Fe/Pb nanocomposite in PRB. Specifically, CIP exhibits a higher affinity for these sites than Cu(II).

3.7.1. Performance of nanocomposite-PRB

The deceleration of CIP and Cu(II) pollutants in the simulated groundwater, which had a Co amount of 0.05 kg/m^3 and a velocity of 0.48 cm/min, was observed upon their arrival at the (QS-Fe/Pb)-PRB. This phenomenon was attributed to the sorption process, which reduced the amount of said pollutants. The amount of pollutants was analyzed in relation to the operational time of (QS-Fe/Pb)-PRB to obtain the theoretical findings for this simulation. Fig. 13 illustrates the correlation between the amount of pollutants leaving (outflow) and entering (inflow) the (QS-Fe/Pb)-PRB at points (33, 25) and (30, 25), respectively, as a function of time. The discrepancy in the contaminant amount escalation between outflow and inflow from the barrier is evident. Implementing the (QS-Fe/Pb)-PRB resulted in a postponement of the increase in outflow of the amount of pollutants by approximately 60 d, in contrast to the inflow of pollutants amounts which was delayed by less than 5 d. This observation suggests that the (QS-Fe/Pb)-PRB effectively impeded contaminants' advancement and delayed their propagation. Furthermore, it is evident that the (QS-Fe/Pb)-PRB exhibits saturation tendencies as travel time increases. This indicates that the efficacy of the nanocomposite-PRB in impeding the migration of pollutants (CIP and Cu(II)) diminishes over time owing to its declining function.

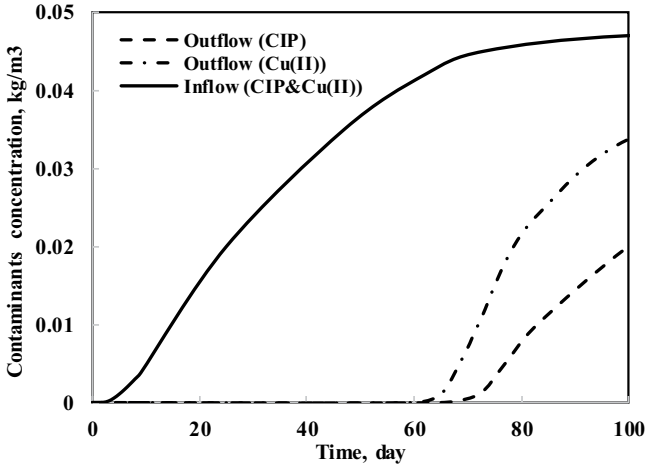

Fig. 13. Contaminants concentrations and time relationship.

3.7.2. Contaminants removal within nanocomposite-PRB

Fig. 14 depicts the relationship between the amount of pollutants and time within the thickness of (QS-Fe/Pb)-PRB. The results indicate a notable disparity in the rate of increase of CIP and Cu(II) amounts between the front and internal areas of the barrier, with the former exhibiting a more rapid increase within a thickness of 1 m. The observed increase in pollutants amount at the leading edge of the barrier indicates a reduction in the efficacy of the reactive material (i.e., QS-Fe/Pb nanocomposite) to remove impurities faster than the inner portion of the barrier.

The observed phenomenon can be attributed to the fact that the frontal segments of the barrier, which have a thickness of 1 m, are exposed to incoming pollutants of significantly higher amounts compared to the inner parts, which have a thickness of 2 and 3 m and receive the same

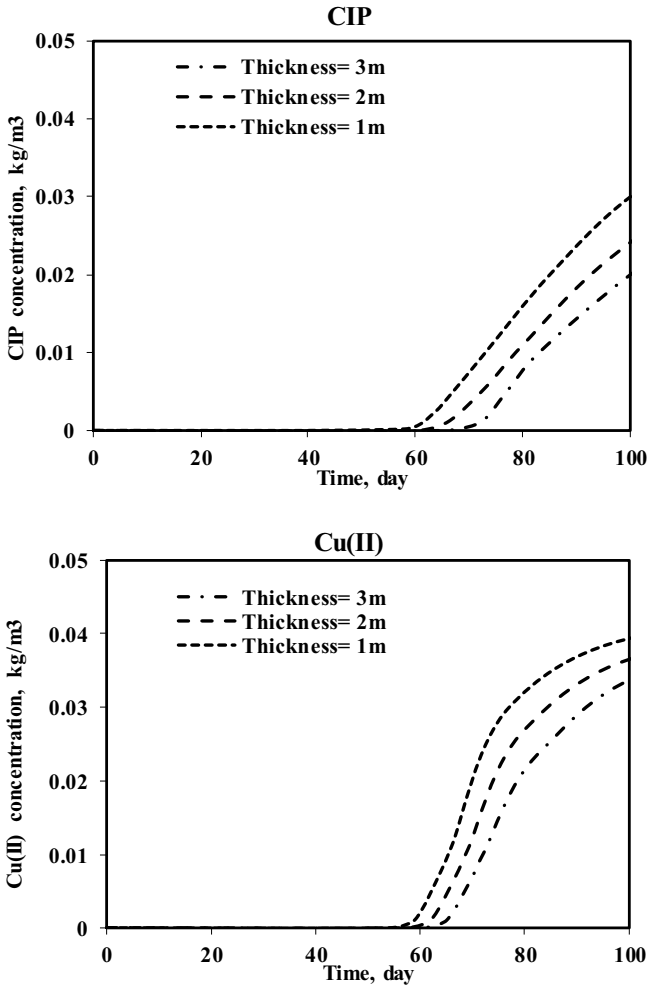

Fig. 14. Contaminants concentration and time relationship within the thickness of barrier.

pollutants but at a lower dose. As a result, the reactive material in the frontal segments reaches its max sorption capacity or becomes saturated earlier, increasing the amount of the pollutants. Conversely, it can be inferred that the reactive material segments situated at the terminal point of the barrier, possessing a thickness of 3 m, would attain their max. sorption capacity or reach saturation at a comparatively delayed juncture compared to the anterior segments. This is because they would be exposed to incoming pollutants with lower amounts for most of the remediation operation.

4. Conclusion

The present investigation utilized an eco-friendly approach by utilizing waste from agriculture as a reducing (anti-oxidant) agent as a replacement for using hazardous chemicals to produce a nanocomposite material (designated as QS-Fe/Pb). The nanocomposite was utilized as a reactive substance in PRB technology to remediate the simulated groundwater contaminated with Cu(II) and CIP through a batch mode of operations. The utilization of batch mode facilitated the exploration of diverse factors, including but not limited to contact duration, initial pH, and nanocomposite dosage. At the operational values of these variables, the maximum percentage of removal observed for Cu(II) and CIP was 99%. The study reports the functional values of various factors. These factors include time durations of 70 and 120 min, numerical values of 7 and 6, a rotational speed of 200 rpm, a concentration of 50 mg/L, and two different quantities of 0.5 g/50 mL and 0.7 g/50 mL. The Freundlich isotherm model demonstrated satisfactory performance in fitting the data about the sorption of Cu(II) and CIP. The adsorption capacity for CIP and Cu(II) was 15 and 9.8 mg/g, respectively. Additionally, the research on sorption kinetics has illuminated that the pseudo-second-order model has provided a more accurate representation of the empirical data, indicating that chemisorption has been the dominant mechanism. The efficacy of the QS-Fe/Pb nanocomposite in impeding the CIP and Cu(II) plume was validated by the two-dimensional aquifer model within the parameters of the present investigation.

References

[1] P.K. Jjemba, Excretion and ecotoxicity of pharmaceutical and personal care products in the environment, Ecotoxicol. Environ. Saf., 63 (2006) 113–130.

[2] B.H. Graimed, Z.T. Abd Ali, Batch and continuous study of one-step sustainable green graphene sand hybrid synthesized from date-syrup for remediation of contaminated groundwater, Alexandria Eng. J., 61 (2022) 8777–8796.

[3] J. Li, L. Pan, G. Yu, S. Xie, C. Li, D. Lai, Z. Li, F. You, Y. Wang, The synthesis of heterogeneous Fenton-like catalyst using sewage sludge biochar and its application for ciprofloxacin degradation, Sci. Total Environ., 654 (2019) 1284–1292.

[4] L.A. Mokif, N.A. Abdulhusain, A low cost material for treatment wastewater contained petroleum pollution, IOP Conf. Ser.: Earth Environ. Sci., 1088 (2022) 012014, doi: 10.1088/1755-1315/1088/1/012014.

[5] O. Falyouna, I. Maamoun, K. Bensaida, Y. Sugihara, O. Eljamal, Removal of Ciprofloxacin From Aqueous Solutions by Nanoscale Zerovalent Iron-Based Materials: A Mini Review, Proceedings of International Exchange and Innovation Conference on Engineering & Sciences (IEICES), 2020, pp. 179–185. Available at: https://doi.org/10.5109/4102485

[6] M. Yoosefian, S. Ahmadzadeh, M. Aghasi, M. Dolatabadi, Optimization of electrocoagulation process for efficient removal of ciprofloxacin antibiotic using iron electrode; kinetic and isotherm studies of adsorption, J. Mol. Liq., 225 (2017) 544–553.

[7] A.M. Michaud, C. Chappellaz, P. Hinsinger, Copper phytotoxicity affects root elongation and iron nutrition in durum wheat (*Triticum turgidum durum* L.), Plant Soil., 310 (2008) 151–165.

[8] Q. Qin, X. Wu, L. Chen, Z. Jiang, Y. Xu, Simultaneous removal of tetracycline and Cu(II) by adsorption and coadsorption using oxidized activated carbon, RSC Adv., 8 (2018) 1744–1752.

[9] Z.T. Abd Ali, Green synthesis of graphene-coated sand (GCS) using low-grade dates for evaluation and modeling of the pH-dependent permeable barrier for remediation of groundwater contaminated with copper, Sep. Sci. Technol., 56 (2021) 14–25.

[10] L.A. Mokif, H.K. Jasim, N.A. Abdulhusain, Petroleum and oily wastewater treatment methods: a mini review, Mater. Today Proc., 49 (2022) 2671–2674.

[11] A.M. Naji, Z.T. Abd Ali, Evaluation of modified bentonite using chemical and physical methods for removal of amoxicillin from aqueous solutions: batch and continuous study, Desal. Water Treat., 294 (2023) 185–201.

[12] O. Al-Hashimi, K. Hashim, E. Loffill, T. Marolt Čebašek, I. Nakouti, A.A.H. Faisal, N. Al-Ansari, A comprehensive review for groundwater contamination and remediation: occurrence, migration and adsorption modelling, Molecules, 26 (2021) 5913, doi: 10.3390/molecules26195913.

[13] Z.T. Abd Ali, Z.Z. Ismail, Experimental and modeling study of water defluoridation using waste granular brick in a continuous up-flow fixed bed, Environ. Eng. Res., 26 (2021) 190506, doi: 10.4491/eer.2019.506.

[14] D.N. Ahmed, L.A. Naji, A.A.H. Faisal, N. Al-Ansari, Mu. Naushad, Waste foundry sand/MgFe-layered double hydroxides composite material for efficient removal of congo red dye from aqueous solution, Sci. Rep., 10 (2020) 1–12.

[15] B.H. Graimed, Z.T. Abd Ali, Green approach for the synthesis of graphene glass hybrid as a reactive barrier for remediation of groundwater contaminated with lead and tetracycline, Environ. Nanotechnol. Monit. Manage., 18 (2022) 100685, doi: 10.1016/j.enmm.2022.100685.

[16] T.H. Mhawesh, Z.T. Abd Ali, Reuse of brick waste as a cheap-sorbent for the removal of nickel ions from aqueous solutions, Iraqi J. Chem. Pet. Eng., 21 (2020) 15–23.

[17] G. Gopal, H. Sankar, C. Natarajan, A. Mukherjee, Tetracycline removal using green synthesized bimetallic nZVI-Cu and bentonite supported green nZVI-Cu nanocomposite: a comparative study, J. Environ. Manage., 254 (2020) 109812, doi: 10.1016/j.jenvman.2019.109812.

[18] B. Sravani, Y.V. Manohara Reddy, J.P. Park, M. Venu, L.S. Sarma, Design of bimetallic PtFe-based reduced graphene oxide as efficient catalyst for oxidation reduction reaction, Catalysts, 12 (2022) 1528, doi: 10.3390/catal12121528.

[19] M. Danish, X. Gu, S. Lu, A. Ahmad, M. Naqvi, U. Farooq, X. Zhang, X. Fu, Z. Miao, Y. Xue, Efficient transformation of trichloroethylene activated through sodium percarbonate using heterogeneous zeolite supported nano zero valent iron-copper bimetallic composite, Chem. Eng. J., 308 (2017) 396–407.

[20] A. Panáček, L. Kvítek, R. Prucek, M. Kolář, R. Večeřová, N. Pizúrová, V.K. Sharma, T. 'jana Nevěčná, R. Zbořil, Silver colloid nanoparticles: synthesis, characterization, and their antibacterial activity, J. Phys. Chem. B, 110 (2006) 16248–16253.

[21] X. Huang, Y. Zhang, D. Zhang, W. Ding, X. Hu, Reduced graphene oxide supported Fe/Ni bimetallic nanoparticles for the rapid adsorption and dechlorination of 2,4-dichlorophenol, Mater. Today Commun., 35 (2023) 105983, doi: 10.1016/j.mtcomm.2023.105983.

[22] G. Gopal, K.V.G. Ravikumar, M. Salma, N. Chandrasekaran, A. Mukherjee, Green synthesized Fe/Pd and *in-situ* bentonite-Fe/Pd composite for efficient tetracycline removal, J. Environ. Chem. Eng., 8 (2020) 104126, doi: 10.1016/j.jece.2020.104126.

[23] R.A. Crane, T.B. Scott, Nanoscale zero-valent iron: future prospects for an emerging water treatment technology, J. Hazard. Mater., 211 (2012) 112–125.

[24] N.A. Abdulhusain, Z.T. Abd Ali, Green approach for fabrication of sand-bimetallic (Fe/Pb) nanocomposite as reactive material for remediation of contaminated groundwater using permeable reactive barrier, Alexandria Eng. J., 72 (2023) 511–530.
[25] N.A. Abdulhusain, Z.T. Abd Ali, Green synthesis of sand-bimetallic Fe/Pb nanoparticles as an environmentally sustainable composite for ciprofloxacin and copper removal from aqueous solutions, Desal. Water Treat., 287 (2023) 155–166.
[26] K.V.G. Ravikumar, S.V. Sudakaran, K. Ravichandran, M. Pulimi, C. Natarajan, A. Mukherjee, Green synthesis of NiFe nano particles using *Punica granatum* peel extract for tetracycline removal, J. Cleaner Prod., 210 (2019) 767–776.
[27] X. Weng, Z. Chen, Z. Chen, M. Megharaj, R. Naidu, Clay supported bimetallic Fe/Ni nanoparticles used for reductive degradation of amoxicillin in aqueous solution: characterization and kinetics, Colloids Surf., A, 443 (2014) 404–409.
[28] K.V.G. Ravikumar, G. Debayan, P. Mrudula, N. Chandrasekaran, M. Amitava, *In-situ* formation of bimetallic FeNi nanoparticles on sand through green technology: application for tetracycline removal, Front. Environ. Sci. Eng., 14 (2020) 1–13.
[29] X. Weng, Q. Sun, S. Lin, Z. Chen, M. Megharaj, R. Naidu, Enhancement of catalytic degradation of amoxicillin in aqueous solution using clay supported bimetallic Fe/Ni nanoparticles, Chemosphere, 103 (2014) 80–85.
[30] A.F. Ali, Z.T. Abd Ali, Sustainable use of concrete demolition waste as reactive material in permeable barrier for remediation of groundwater: batch and continuous study, J. Environ. Eng., 146 (2020) 4020048, doi: 10.1061/(ASCE)EE.1943-7870.0001714.
[31] B. des Faulverhaltens, German Standard Methods for the Examination of Water, Wastewater and Sludge; Sludge and Sediments (Group S); Determination of the Amenability to Anaerobic Digestion (S 8), Ger. Inst. Stand. Berlin, Ger. 1985.
[32] M.N. Ezzat, Z.T. Abd Ali, Green approach for fabrication of graphene from polyethylene terephthalate (PET) bottle waste as reactive material for dyes removal from aqueous solution: batch and continuous study, Sustainable Mater. Technol., 32 (2022) e00404, doi: 10.1016/j.susmat.2022.e00404.
[33] Z.T. Abd Ali, Green synthesis of graphene-coated glass as novel reactive material for remediation of fluoride-contaminated groundwater, Desal. Water Treat., 226 (2021) 113–124.
[34] A.H. Sulaymon, Z.T. Abd Ali, Removal of kerosene from waste water using Iraqi bentonite, J. Eng., 16 (2010) 5422–5437.
[35] Z.T. Abd Ali, Combination of the artificial neural network and advection-dispersion equation for modeling of methylene blue dye removal from aqueous solution using olive stones as reactive bed, Desal. Water Treat., 179 (2020) 302–311.
[36] N. Saad, Z.T. Abd Ali, L.A. Naji, A.A.A.H. Faisal, N. Al-Ansari, Development of Bi-Langmuir model on the sorption of cadmium onto waste foundry sand: effects of initial pH and temperature, Environ. Eng. Res., 25 (2020) 677–684.
[37] H.J. Khadim, F.K. Obaed, Z.T. Abd Ali, Application of MQ-Sensors to Indoor Air Quality Monitoring in Lab based on IoT, International Conference on Intelligent Technology, System and Service for Internet of Everything (ITSS-IoE), IEEE, Sana'a, Yemen, 2021, pp. 1–5.
[38] N.A. Abdulhusain, L.A. Mokif, The removal performance of bio-sorption on sunflower seed husk for copper and lead ions from aqueous solutions, J. Ecol. Eng., 24 (2023) 110–117.
[39] B.H. Graimed, Z.T. Abd Ali, Thermodynamic and kinetic study of the adsorption of Pb(II) from aqueous solution using bentonite and activated carbon, Al-Khwarizmi Eng. J., 9 (2013) 48–56.
[40] Z.T. Abd Ali, H.J. Khadim, M.A. Ibrahim, Simulation of the remediation of groundwater contaminated with ciprofloxacin using grafted concrete demolition wastes by ATPES as reactive material: batch and modeling study, Egypt. J. Chem., 65 (2022) 585–596.
[41] Z.T. Abd Ali, Using activated carbon developed from iraqi date palm seeds as permeable reactive barrier for remediation of groundwater contaminated with copper, Al-Khwarizmi Eng. J., 12 (2016) 34–44.
[42] M. Khebchareon, Crank–Nicolson finite element for 2-D groundwater flow, advection-dispersion and interphase mass transfer: I. model development, Int. J. Numer. Anal. Model. Ser. B, 3 (2012) 109–125.
[43] C.C. Travis, G.F. Webb, Cosine families and abstract nonlinear second order differential equations, Acta Math. Hungarica, 32 (1978) 75–96.
[44] L. Du, L. Luo, Z. Feng, M. Engelhard, X. Xie, B. Han, J. Sun, J. Zhang, G. Yin, C. Wang, Nitrogen–doped graphitized carbon shell encapsulated NiFe nanoparticles: a highly durable oxygen evolution catalyst, Nano Energy, 39 (2017) 245–252.
[45] Z.-J. Li, L. Wang, L.-Y. Yuan, C.-L. Xiao, L. Mei, L.-R. Zheng, J. Zhang, J.-H. Yang, Y.-L. Zhao, Z.-T. Zhu, Efficient removal of uranium from aqueous solution by zero-valent iron nanoparticle and its graphene composite, J. Hazard. Mater., 290 (2015) 26–33.
[46] S. Kango, R. Kumar, Magnetite nanoparticles coated sand for arsenic removal from drinking water, Environ. Earth Sci., 75 (2016) 1–12.
[47] A.M. Osman, A.H. Hendi, T.A. Saleh, Simultaneous adsorption of dye and toxic metal ions using an interfacially polymerized silica/polyamide nanocomposite: kinetic and thermodynamic studies, J. Mol. Liq., 314 (2020) 113640, doi: 10.1016/j.molliq.2020.113640.
[48] J. Liu, Y. Du, W. Sun, Q. Chang, C. Peng, A granular adsorbent-supported Fe/Ni nanoparticles activating persulfate system for simultaneous adsorption and degradation of ciprofloxacin, Chin. J. Chem. Eng., 28 (2020) 1077–1084.
[49] D. Wang, J. Li, Z. Xu, Y. Zhu, G. Chen, Preparation of novel flower-like $BiVO_4/Bi_2Ti_2O_7/Fe_3O_4$ for simultaneous removal of tetracycline and Cu^{2+}: adsorption and photocatalytic mechanisms, J. Colloid Interface Sci., 533 (2019) 344–357.
[50] G. Lamzougui, A. Es-Said, H. Nafai, D. Chafik, A. Bouhaouss, R. Bchitou, Optimization and modeling of Pb(II) adsorption from aqueous solution onto phosphogypsum by application of response surface methodology, Phosphorus, Sulfur Silicon Relat. Elem., 196 (2021) 521–529.
[51] J. Jin, Z. Yang, W. Xiong, Y. Zhou, R. Xu, Y. Zhang, J. Cao, X. Li, C. Zhou, Cu and Co nanoparticles co-doped MIL-101 as a novel adsorbent for efficient removal of tetracycline from aqueous solutions, Sci. Total Environ., 650 (2019) 408–418.
[52] Y. Lin, X. Jin, G. Owens, Z. Chen, Simultaneous removal of mixed contaminants triclosan and copper by green synthesized bimetallic iron/nickel nanoparticles, Sci. Total Environ., 695 (2019) 133878, doi: 10.1016/j.scitotenv.2019.133878.
[53] L. Chen, T. Yuan, R. Ni, Q. Yue, B. Gao, Multivariate optimization of ciprofloxacin removal by polyvinylpyrrolidone stabilized nZVI/Cu bimetallic particles, Chem. Eng. J., 365 (2019) 183–192.
[54] L. Chen, R. Ni, T. Yuan, Y. Gao, W. Kong, P. Zhang, Q. Yue, B. Gao, Effects of green synthesis, magnetization, and regeneration on ciprofloxacin removal by bimetallic nZVI/Cu composites and insights of degradation mechanism, J. Hazard. Mater., 382 (2020) 121008, doi: 10.1016/j.jhazmat.2019.121008.
[55] G. Gopal, C. Natarajan, A. Mukherjee, Synergistic removal of tetracycline and copper(II) by *in-situ* B-Fe/Ni nanocomposite—a novel and an environmentally sustainable green nanomaterial, Environ. Technol. Innovation, 25 (2022) 102187, doi: 10.1016/j.eti.2021.102187.
[56] O. Falyouna, I. Maamoun, K. Bensaida, A. Tahara, Y. Sugihara, O. Eljamal, Encapsulation of iron nanoparticles with magnesium hydroxide shell for remarkable removal of ciprofloxacin from contaminated water, J. Colloid Interface Sci., 605 (2022) 813–827.
[57] A.A. Naji, Z.T. Abd Ali, A single-step method as a green approach to fabricate magnetite nanocomposite for removal of moxifloxacin and cadmium from aqueous solutions, Environ. Nanotechnol. Monit. Manage., 20 (2023) 100883, doi: 10.1016/j.enmm.2023.100883.
[58] Z.B. Masood, Z.T.A. Ali, Numerical modeling of two-dimensional simulation of groundwater protection from lead using different sorbents in permeable barriers, Environ. Eng. Res., 25 (2020) 605–613.
[59] A.A.H. Faisal, Z.T. Abd Ali, Phenol removal using granular dead anaerobic sludge permeable reactive barrier in a simulated groundwater pilot plant, J. Eng., 20 (2014) 63–79.